

Borehole Temperatures and a Baseline for 20th-Century Global Warming Estimates

Robert N. Harris* and David S. Chapman

Lack of a 19th-century baseline temperature against which 20th-century warming can be referenced constitutes a deficiency in understanding recent climate change. Combination of borehole temperature profiles, which contain a memory of surface temperature changes in previous centuries, with the meteorological archive of surface air temperatures can provide a 19th-century baseline temperature tied to the current observational record. A test case in Utah, where boreholes are interspersed with meteorological stations belonging to the Historical Climatological Network, yields a noise reduction in estimates of 20th-century warming and a baseline temperature that is $0.6^\circ \pm 0.1^\circ\text{C}$ below the 1951 to 1970 mean temperature for the region.

Analysis of surface air temperature (SAT) measurements provides the primary evidence for recent and widespread climatic warming and indicates that the average global warming since 1900 has been $0.45^\circ \pm 0.15^\circ\text{C}$ (1, 2). The SAT record, however, is short; very few records extend back to 1870. It is therefore unclear whether observed 20th-century warming is part of a natural cycle, representing a return to normal, or whether it represents an anthropogenic-induced departure from some cooler natural state (3). In spite of the importance of these contrasting histories, it is not possible to discriminate between such scenarios from SAT data alone. Knowledge of a baseline preindustrial surface temperature from which the record of modern SAT warming can be referenced might help to discriminate between these contrasting views. Additionally, a baseline preindustrial surface temperature could either support or weaken the apparent correlation between concentrations of greenhouse gases and observed warming (1, 2).

Subsurface temperature records in the solid Earth may solve this problem. Because rock has a relatively low thermal diffusivity, changes in temperature at the Earth's surface propagate slowly downward into the Earth, perturbing the background temperature field. Excursions in average surface temperature 10, 100, and 1000 years ago produce maximum temperature anomalies at depths of 25, 80, and 250 m, respectively, in the subsurface temperature field today. Therefore, the last millennium of surface temperature change is potentially recoverable from detailed temperature-depth logs in boreholes. Heat conduction unfortunately smears the climate signal but still leaves a thermally averaged and robust signal of long-period temperature vari-

ations at the Earth's surface. The deeper the transient temperature perturbation, the longer the span of temperature history it represents (4).

Many analyses of borehole temperature-depth profiles (5) have shown that warming began 50 to 200 years ago, is correlated with latitude, and is generally consistent with predictions from General Circulation Models (6). A few regional (7–11) or site-specific

(12) studies have linked meteorological and geothermal data. Utah's setting is ideal for combining these two data types because high-quality temperature-depth logs are available for sites where hydrologic, terrain, and cultural disturbances to the subsurface temperature field are minimal, and meteorological stations with long observing times are geographically interspersed with the borehole sites.

We used two sets of geothermal data, one from southeastern Utah (13) and the other from western Utah (14). Boreholes in southeastern Utah penetrate sedimentary rocks, extend to depths of 300 to 500 m, and were measured between 1979 and early 1980. Boreholes in western Utah penetrate crystalline rocks, are 150 m deep, and were measured in 1978.

In reconstructing surface temperature histories (Fig. 1), we first estimated a background, quasi-steady-state temperature field from the raw temperature-depth measurements (Fig. 1A) using a least-squares functional space inverse algorithm (15). Removal of this background temperature field gives our best estimate of the transient signal (Fig. 1B). Reduced temperatures near the surface are systematically positive, have an amplitude of

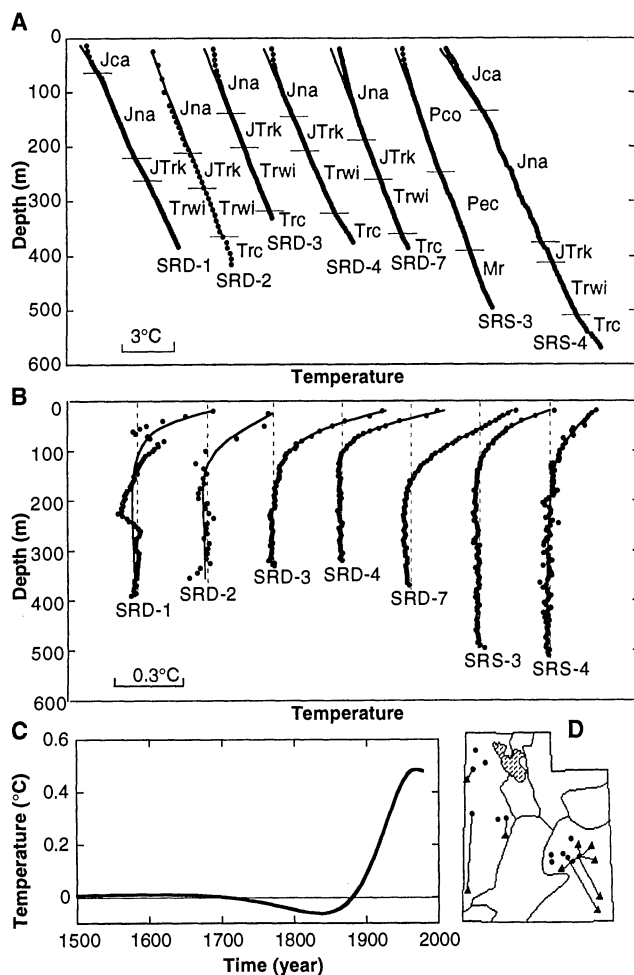


Fig. 1. Borehole temperature-depth data and surface ground temperature (SGT) reconstructions for southeastern Utah. **(A)** Raw temperature-depth data. Individual temperature measurements (circles) and background temperature field (lines). Temperatures are offset to avoid overlap. Sedimentary formation abbreviations: Jca (Carmel), Jna (Navajo), JTrk (Kayenta), Trwi (Wingate), Trc (Chinle), Pco (Coconino), Pec (Elephant Canyon). **(B)** Reduced temperatures (circles) are obtained by subtracting background thermal field from raw temperature-depth measurements. Solid lines show transient temperatures ascribed to a changing ground-surface condition. **(C)** Average SGT history. **(D)** Location map of Utah in the western United States showing meteorological stations (triangles) from the Historical Climatology Network and borehole sites (circles). Lines between meteorological stations and boreholes show preferred ties. Climatic divisions in Utah are also marked.

Department of Geology and Geophysics, University of Utah, Salt Lake City, UT 84112, USA.

*To whom correspondence should be addressed. E-mail: rnharris@mines.utah.edu

0.2° to 0.5°C, and a depth extent of between 100 and 200 m. Variations among reduced temperature profiles reflect natural variability and local climatological effects. High-frequency variations may indicate small thermal conductivity deviations or thermal instabilities in the boreholes (10).

Because anomalous or reduced temperatures in boreholes can arise from nonclimatic sources, we considered other possible sources of temperature perturbations such as the effects of variable thermal conductivity or heat production, and the effects of topography, erosion, burial, and groundwater flow at each site. All of these effects were found to be negligible at the noise level of the data (8, 16, 17). For these boreholes, long-wavelength departures from a background temperature field are best explained by changing surface temperatures with time.

The surface ground temperature (SGT) reconstructed for a particular time τ before the borehole temperature measurement represents a time average over $\pm 0.6\tau$ centered on that time. Thus, SGT histories represent a series of time-averaged temperatures with an increasing averaging window as we look farther into the past (18). The average SGT history for this suite of boreholes (19) (Fig. 1C) suggests time-averaged temperatures that were relatively constant to 1750, slightly decreasing to 1850, warmed by

0.6°C to 1960, and were stable to 1978.

We now combine SAT records, from the Historical Climatology Network (HCN) (20), with the geothermal record of surface temperature variations. Borehole temperatures and air column temperatures are both direct, but independent, measures of surface temperature and its change through time. SATs respond to convective heat transfer in an atmospheric boundary layer and represent discrete measurements at fixed times of the day. In contrast, transient temperatures in the solid Earth represent a continuously integrated history of ground temperature variations near the borehole. Several studies have demonstrated that synthetic temperature-depth profiles computed through the use of SAT records from nearby weather stations as forcing functions at Earth's surface reproduce many features of borehole temperature profiles (7–11, 16).

SAT time series and borehole transient temperatures can be explicitly correlated by modeling Earth's response to surface temperature changes as recorded in SAT time series. Synthetic transient temperature profiles can be computed by expressing annual mean SAT time series in terms of a series of step functions. For a surface temperature history $\Delta T(0, \tau)$ composed of n individual step changes in surface temperature of amplitude ΔT_i and time τ_i before the borehole temperature measurement, transient temperatures at the time of measurement can be expressed as (21)

$$\Delta T(z) = \sum_{i=1}^n \Delta T_i \operatorname{erfc}\left(\frac{z}{\sqrt{4\alpha\tau_i}}\right) \quad (1)$$

where erfc is the complementary error function and α is thermal diffusivity. However, to perform this calculation, a long-term or preobservational mean (POM) surface temperature before the onset of SAT measurements must be estimated (7, 9). The POM can be written explicitly in terms of the first step change in temperature, where $\Delta T_1 = (T_1 - \text{POM})$ and τ_1 is the onset time of the first annual mean. In practice, the POM is determined by finding the value that minimizes the misfit between the reduced temperatures and the synthetic transient temperatures computed from the SAT record. This is a robust comparison as there is only one free parameter, and where temperature perturbations do not result from variations in surface temperature, the correlation between SAT time series and reduced temperatures will be poor, despite the choice of POM.

We illustrate this technique for the HCN weather station at Green River, Utah, linked to the borehole site SRD-4, logged in 1979. Departures from the 1951 to 1970 mean SAT at Green River for the time period 1911 to 1979 (Fig. 2A) are used as a forcing function to compute synthetic transient temperature-depth profiles. Three choices of POM, each separated by 0.6°C, are shown and quoted relative to the 1951 to 1970 mean value: a POM I of 0.0°C representative

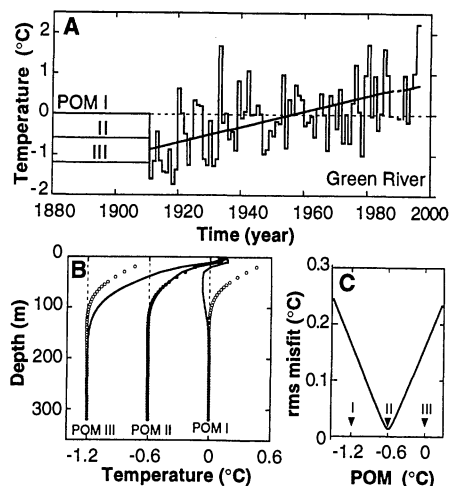


Fig. 2. Determination of the preobservational mean (POM). (A) Mean annual departures of SAT data for Green River for the period 1911 to 1994 plotted relative to the 1951 to 1970 mean (dashed line). Linear fit to data yields a warming trend of 1.8°C per 100 years. Horizontal lines marked POM I, II, and III illustrate three possible choices of POM. (B) Three synthetic transient temperature-depth profiles constructed with the use of SAT data from Green River coupled with a corresponding choice of POM from (A) (solid lines). Temperature perturbation for borehole SRD-4 (circles) is plotted relative to each POM. (C) Root-mean-square misfit as a function of the POM illustrating the best fit for POM II.

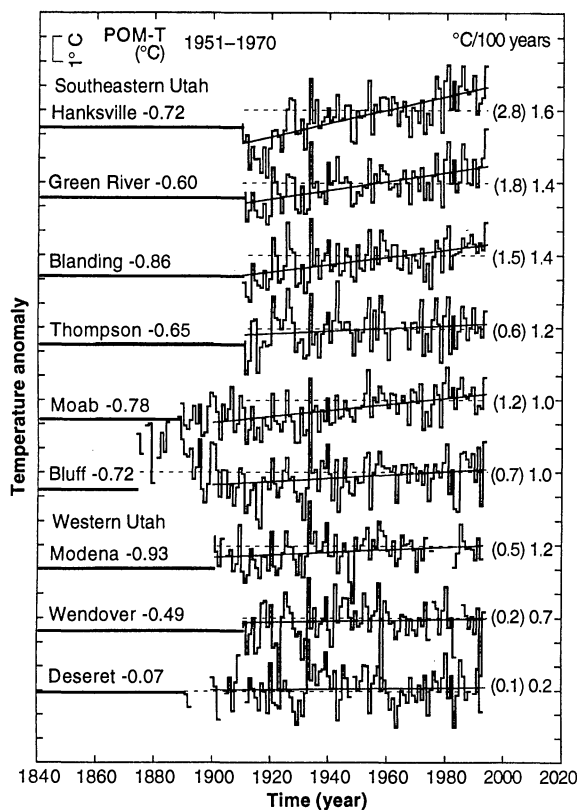


Fig. 3. Preferred POM or baseline temperature shown with SAT time series and linear trends. Top six time series are from southeastern Utah and are adjusted for both time-of-observation bias and nonclimatic biases; bottom three time series are from western Utah and are adjusted for time-of-observation bias only (22). Linear century trends (°C per 100 years) are computed from SAT data alone (parentheses) and from SAT data constrained by the POM.

of the 1951 to 1970 mean temperature; a POM II of -0.6°C , representative of average temperatures in the first half of this century; and a POM III of -1.2°C that would constitute an extreme long-term warming scenario. We calculated synthetic transient temperature profiles (solid lines in Fig. 2B) by coupling a particular value of the POM with the SAT data. For the highest initial temperature scenario (POM I in Fig. 2A), the SAT record is cooler on average than POM I for the early part of this century; the synthetic transient temperature profile therefore shows a cooling inflection at a depth of about 150 m. Predicted transient temperatures are zero or negative for most of the borehole. In contrast, for the lowest POM value (POM III), the SAT record is warmer than the baseline temperature, and the synthetic transient profile shows a distinctive warming profile.

An intermediate value of -0.6°C (POM II) produces the transient that most closely matches the reduced temperature data (open circles). Baseline temperatures, POM I and POM III, can be excluded with considerable certainty (Fig. 2B). Furthermore, the reduced temperature and transient signals correlate well in both amplitude and depth. For this example, the SAT 1951 to 1970 mean value is 11.0°C , and thus we infer that the baseline temperature at Green River before 1911 was $10.4 \pm 0.1^{\circ}\text{C}$.

We calculated root-mean-square (rms) misfits for each possible meteorological-borehole combination to determine the best ties. In southeastern Utah, where the boreholes extend to variable depths, the rms misfit was calculated to depths $z = 2\sqrt{4\alpha\tau}$, where τ is the time between the first annual mean and the year the data were collected for that particular meteorological station. This practice avoids biasing ties toward the deeper boreholes. In western Utah, where all the boreholes are the same depth (150 m), we used the entire reduced temperature profile to calcu-

late the rms difference. In most cases, preferred ties between borehole sites and meteorological stations, as guided by minimum rms misfits, are also close (Fig. 1D). Our results show that a POM coupled with SAT measurements from a nearby meteorological site explains greater than 90% of the transient borehole temperature signal. These results suggest that ground temperatures are faithfully tracking changes in temperature at the Earth's surface at the Utah sites (22).

Baseline temperatures relative to the average 1951 to 1970 SAT mean temperature for six meteorological/borehole pairs (Fig. 3 and Table 1) from southeastern Utah vary between -0.60°C and -0.86°C with an average of -0.72°C relative to the 1951 to 1970 mean SAT and have a group SD of 0.09°C . SAT century warming trends at individual stations are highly variable, ranging from $+2.8^{\circ}\text{C}$ per 100 years for Hanksville to $+0.7^{\circ}\text{C}$ per 100 years for Bluff; the group SD is 0.8°C . In contrast, century-long trends constrained to pass through the POM at the beginning of the SAT record show less variability, with a SD of 0.4°C , 50% less than the SD of the linear fits on the basis of SAT data alone. As shown in Fig. 3, several HCN stations in southeastern Utah with high apparent temperature change this century (Hanksville, Green River, Moab) overestimate the surface temperature change inferred from the combined geothermal meteorological data analysis. For the small sample in western Utah, the average POM is -0.50°C (SD = 0.4°C). In this area, HCN stations with low apparent temperature change (Modena and Wendover) underestimate the surface temperature change this century.

These POM or baseline temperatures preclude that 20th-century warming is simply a recovery to normal conditions from an abnormally cool period at the beginning of this century. Likewise, baseline temperatures in Utah were not much cooler than those prevailing at the turn of the century. The data,

instead, support a baseline temperature that is consistent with the ~ 1900 SATs. For southeastern Utah, the magnitude of warming from 19th-century baseline to 1951 to 1970 is 0.6°C ; extension to include the most recent warming yields a total of 1.0°C warming to the 1990 to 1994 mean.

REFERENCES AND NOTES

1. J. Hansen and S. Lebedeff, *J. Geophys. Res.* **92**, 13345 (1987).
2. P. D. Jones, T. M. L. Wigley, K. R. Briffa, in *Trends '93: A Compendium of Data on Global Change*, T. A. Boden, D. P. Kaiser, R. J. Sepanski, F. W. Stoss, G. M. Logsdon, Eds. (Carbon Dioxide Information Analysis Center, Oak Ridge National Laboratory, Oak Ridge, TN, 1994), pp. 603–608.
3. H. W. Ellsaesser, M. C. MacCraken, J. J. Walton, S. L. Grotch, *Rev. Geophys.* **24**, 745 (1986).
4. A. H. Lachenbruch and B. V. Marshall, *Science* **234**, 689 (1986); H. N. Pollack and D. S. Chapman, *Sci. Am.* **268**, 44 (June 1993).
5. D. Deming, *Science* **268**, 1576 (1995).
6. T. M. L. Wigley and T. P. Barnett, in *Climate Change: The IPCC Scientific Assessment*, J. T. Houghton, C. J. Jenkins, J. J. Ephraums, Eds. (Cambridge Univ. Press, Cambridge, 1990), pp. 239–255.
7. A. H. Lachenbruch, T. T. Cladouhos, R. W. Saltus, paper presented at the 5th International Conference on Permafrost, Trondheim, Norway, August 1988.
8. T. J. Chisholm, and D. S. Chapman, *J. Geophys. Res.* **97**, 14155 (1992).
9. D. S. Chapman, T. J. Chisholm, R. N. Harris, *Palaeogeogr. Palaeoclimatol. Palaeoecol.* **98**, 269 (1992).
10. D. S. Chapman and R. N. Harris, *Geophys. Res. Lett.* **18**, 1891 (1993).
11. W. D. Gosnold, P. E. Todhunter, W. Schmidt, in preparation.
12. S. N. Putnam and D. S. Chapman, *J. Geophys. Res.* **101**, 21877 (1996).
13. J. M. Bodell and D. S. Chapman, *ibid.* **87**, 2869 (1982).
14. D. S. Chapman *et al.*, *U.S. Geol. Surv. Final Rep. 14-08-001-G-341* (1978), vol. 2.
15. This formulation is based on one-dimensional heat conduction in a layered half-space with a temperature-depth distribution assumed to be composed of (i) a steady-state component governed by the long-term mean surface ground temperature, basal heat flow, and thermophysical properties of the rocks in which the temperature measurements are made; and (ii) a transient component assumed to be caused by time variations of the ground surface temperature [P. Y. Shen and A. E. Beck, *J. Geophys. Res.* **96**, 19965 (1991)]. Solutions are stabilized and uniquely determined by incorporating estimates and uncertainties about the thermophysical model parameters and representation errors stemming from representing the Earth with a one-dimensional model [P. Y. Shen, H. N. Pollack, S. Huang, K. Wang, *J. Geophys. Res.* **100**, 6383 (1995)]. Thermal conductivity, radiogenic heat production, and thermal diffusivity values for southeastern and western Utah have been reported (10, 18). A good trade-off between solution resolution and variance is achieved for a priori SDs of $\sigma_{k_0} = 2.0 \text{ W m}^{-1} \text{ K}^{-1}$ and $\sigma_{d_0} = 50 \text{ mK}$ for southeastern Utah, and $\sigma_{k_0} = 1.0 \text{ W m}^{-1} \text{ K}^{-1}$ and $\sigma_{d_0} = 50 \text{ mK}$ for western Utah, where σ_{k_0} and σ_{d_0} represent a priori SDs of thermal conductivity and temperature-depth data, respectively. The larger σ_{k_0} value for southeastern Utah compensates for the increased variability of thermal conductivities (and other thermophysical rock properties) associated with the layered sedimentary strata in which these temperature-depth measurements were made.
16. R. N. Harris and D. S. Chapman, *J. Geophys. Res.* **100**, 6367 (1995).
17. _____, in preparation.
18. G. D. Clow, *Palaeogeogr. Palaeoclimatol. Palaeoecol.* **98**, 81 (1992).
19. Averaging solutions is equivalent to a simultaneous

Table 1. Fits between meteorological stations and boreholes. SAT average is based on 1951 to 1970 mean annual temperatures. POM, preobservational mean; rms, root-mean-square misfit between the reduced temperatures and the best fitting SAT-POM model (22).

Meteorological station/borehole	Borehole depth (m)	SAT average ($^{\circ}\text{C}$)	Linear fit ($^{\circ}\text{C}$ per 100 years)	POM ($^{\circ}\text{C}$)	rms (mK)
<i>Southeastern Utah</i>					
Green River/SRD-4	320	10.90	+1.8	-0.60	11
Thompson/SRD-3	330	11.20	+0.6	-0.65	12
Moab/SRD-4	320	13.15	+1.2	-0.78	13
Hanksville/SRD-4	330	11.15	+2.8	-0.72	15
Blanding/SRD-3	330	10.13	+1.5	-0.86	14
Bluff/SRD-7	370	11.81	+0.7	-0.72	12
<i>Western Utah</i>					
Wendover/SI-1	150	11.26	+0.2	-0.49	10
Modena/DC-1	150	9.26	+0.5	-0.93	16
Deseret/DM-1	150	9.10	+0.1	-0.07	16

inversion and enhances the long-period signal of regional climate change [H. N. Pollack, P. Y. Shen, S. Huang, *Pure Appl. Geophys.* **147**, 537 (1996)].

20. Stations comprising the HCN have the properties of a relatively long temperature series, a predominantly undisturbed environment around the meteorological site, and limited station relocations [D. R. Easterling, T. R. Karl, E. H. Mason, P. Y. Hughes, D. P. Bowman, *United States Historical Climatology Network (U.S. HCN) Monthly Temperature and Precipitation Data. ORNL/CDIAC-87, NDP-019/R3* (Carbon Dioxide Information Analysis Center, Oak Ridge National Laboratory, Oak Ridge, TN, 1996)].

21. H. S. Carslaw and J. C. Jaeger, *Conduction of Heat in Solids* (Oxford Univ. Press, New York, 1959).

22. The HCN data set contains raw SAT (SAT_{raw}) data as well as data adjusted for time-of-observation biases (SAT_{tob}) and data adjusted for both the time-of-observation-biases and nonclimatic biases (SAT_{ncb}).

The time-of-observation bias, owing to different observation schedules, is adjusted on the basis of an empirical model [T. R. Karl, C. N. Williams Jr., P. J. Young, W. M. Wendland, *J. Climate* **25**, 145 (1986)]. Nonclimatic biases resulting from instrument changes and station relocations are adjusted on the basis of correlations between a candidate station and its 20 closest neighbors [T. R. Karl and C. N. Williams Jr., *J. Climate* **26**, 1744 (1987)]. In southeastern Utah, the average misfit between transient temperatures and synthetic transients for the preferred ties is 30, 25, and 9 mK for SAT_{raw} , SAT_{tob} , and SAT_{ncb} , respectively. These misfits illustrate the progression one would expect; each succeeding correction brings the SAT data and transient temperatures into better agreement. In western Utah, however, average rms misfits between the transient temperatures and the synthetic transients are 16, 6, and 21 mK for the SAT_{raw} , SAT_{tob} , and SAT_{ncb} , respectively. This

implies that whereas the time-of-observation bias adjustment improves the correlation between the SAT time series and the transient borehole temperatures, the nonclimatic bias adjustment does not. Because meteorological stations in western Utah fall in an area of extremely sparse coverage, the nonclimatic bias correction is not as well constrained as in areas where station density is greater. In this study, we use SAT_{ncb} and SAT_{tob} for southeastern and western Utah, respectively.

23. We thank A. H. Lachenbruch, whose early work on climate reconstruction from borehole temperatures stimulated parts of this study, for providing constructive comments. Supported by the National Science Foundation (EAR-9104292 and EAR-9205031) and grant project No. 92037 of the Czech-U.S. Science and Technology Cooperation Program.

8 November 1996; accepted 14 January 1997

High-Pressure Iron-Sulfur Compound, Fe_3S_2 , and Melting Relations in the Fe-FeS System

Yingwei Fei,* Constance M. Bertka, Larry W. Finger

An iron-sulfur compound (Fe_3S_2) was synthesized at pressures greater than 14 gigapascals in the system Fe-FeS. The formation of Fe_3S_2 changed the melting relations from a simple binary eutectic system to a binary system with an intermediate compound that melted incongruently. The eutectic temperature in the system at 14 gigapascals was about 400°C lower than that extrapolated from Usselman's data, implying that previous thermal models of Fe-rich planetary cores could overestimate core temperature. If it is found in a meteorite, the Fe_3S_2 phase could also be used to infer the minimum size of a parent body.

Cosmochemical and geophysical arguments (1) suggest that sulfur (S) may be the lighter alloying element in the Fe-rich cores of planets such as the Earth and Mars. Because the Earth consists of a liquid outer core and a solid inner core, the melting relations in the system Fe-FeS at high pressure (P) are used to estimate the core temperature (T). For Mars, we do not know if the core is solid or liquid. The melting relations could place a constraint on the state of the core for a given composition and core T . The eutectic melting T is used to evaluate the efficiency of Fe-rich core segregation in early core formation processes. Many models of core T and core formation processes were based on extrapolation of melting data in the system Fe-FeS obtained at relatively low P (<10 GPa) (2-4). The extrapolations were based on an assumption that no intermediate compound formed in the system, and therefore the melting behavior could be predicted based on simple thermodynamic relations. We report a Fe-S compound formed at $P > 14$ GPa, which changes the melting relations in the Fe-FeS system.

Geophysical Laboratory and Center for High Pressure Research, Carnegie Institution of Washington, 5251 Broad Branch Road, NW, Washington, DC 20015, USA.

*To whom correspondence should be addressed. E-mail: fei@gl.ciw.edu

Iron and FeS form a binary system at ambient P with a eutectic melting point at 988°C and 31% S (all percentages are given by weight) (5). The eutectic composition becomes more Fe-rich with increasing P , whereas the eutectic T remains nearly constant to at least 6 GPa (2-4). At $P > 6$ GPa, Usselman (2) reported that the eutectic T rose with a slope of ~ 34 K/GPa to at least 10 GPa. We conducted melting experiments in the Fe-FeS system in a multi-anvil apparatus (6) to a P higher than that of (2). The experimentally determined eutectic T and composition in this study are in good agreement with previous studies (2-4) to 5 GPa. Eutectic melting was determined on the basis of quenched textures, similar to those described in (2-4), and composition maps. At $P < 14$ GPa, the

quenched textures and compositions are due to eutectic melting in the Fe-FeS binary system in which two solids, Fe and FeS, coexist below the eutectic T (Fig. 1A), whereas one solid FeS (or Fe, depending on the composition of the starting material) and a liquid phase coexist between the eutectic and liquidus T 's (Fig. 1B). The composition of the liquid at the eutectic T represents the eutectic composition of the system. The S content of the eutectic linearly decreases with increasing P , from 31% S at 1 bar to $20.7 \pm 0.4\%$ S at 7 GPa, consistent with (3, 4). Pressure has very little effect on the eutectic composition between 7 and 14 GPa. The eutectic T linearly decreased with increasing P , from 988°C at 1 bar to 860°C at 14 GPa, contrary to the results of Usselman (2), who reported a cusp in the eutectic curve at 5.2 GPa. Our eutectic T at 10 GPa was about 200°C less than that of Usselman at the same P .

At $P > 14$ GPa, we found a Fe-S compound, Fe_3S_2 ($27.9 \pm 0.3\%$ S) (7). An intergrowth of metallic Fe and Fe_3S_2 was quenched from runs with P between 14 and 18 GPa and T of less than the eutectic T (Fig. 1C), when starting materials with 16.1 and 22.3% S were used. At $T = 875^\circ\text{C}$ and $P = 14$ GPa, Fe_3S_2 coexisted with a eutectic liquid composition ($18.2 \pm 0.3\%$ S) (Fig. 1D). When comparing the results from the two unmelted runs at 10 and 14 GPa (Fig. 1, A and C), it is evident that

Table 1. Crystallographic parameters for the phases found in the quenched sample of Fe_3S_2 . The numbers in parentheses are the errors in the last digits.

Quantity (unit)	Troilite	α -Fe	Monoclinic	Triclinic
a (Å)	5.9656(7)	2.8676(5)	5.0481(9)	2.372(1)
b (Å)	5.9656(7)	2.8676(5)	4.436(1)	3.427(1)
c (Å)	11.757(6)	2.8676(5)	4.387(1)	5.999(4)
α	90	90	90	82.09(2)
β	90	90	99.75(1)	79.50(6)
γ	120	90	90	73.99(4)
V (Å ³)	362.4(2)	23.58(1)	96.84(2)	45.90(2)